



Cluster dynamics, growth and syneresis during silica hydrogel polymerisation

David J.S. Birch^{*}, Chris D. Geddes

The Photophysics Group, Department of Physics and Applied Physics, Strathclyde University, John Anderson Building, 107 Rottenrow, Glasgow G4 0NG, UK

Received 10 January 2000; in final form 7 February 2000

Abstract

The aggregation and syneresis of silica particles during hydrogel polymerisation has been observed in situ for the first time with near-Å resolution using a new approach based on the combined fluorescence anisotropy decay of solvated and bound dye molecules. Primary particles of mean hydrodynamic diameter ~ 1.5 nm are found to be present within 20 min of mixing sodium silicate solution and sulphuric acid. Clustering then occurs during siloxane polymerisation to produce after ~ 30 h secondary particles with a mean diameter up to ~ 4.5 nm at a growth rate which depends on silicate concentration and time to microgelation, t_g . Subsequent condensation to ~ 4 nm diameter occurs within 1 week as particle syneresis dominates. The effects on particle growth of adding D_2O and inorganic salts are demonstrated. © 2000 Elsevier Science B.V. All rights reserved.

There can be few more important materials than silica and water. The former constitutes the most abundant material in the Earth's crust and the latter occupies most of the surface of the Earth. The properties of the two are inextricably linked in the search for a better understanding of the molecular dynamics responsible for sol to gel phase transitions. Few techniques permit the study of both, but in this Letter we report the results of a new approach which gives independent, simultaneous and in situ characterisation of the aqueous phase and silica particle size during sol–gel polymerisation.

The sol–gel process is a room-temperature inorganic polymerisation involving a series of hydrolysis and condensation steps to produce a rigid network and which owes its origins to the pioneering work of Ebelman, Mendelejev and Graham in the 19th century [1]. The sol to gel transition is characterised by a gel point, after a time t_g , at which a fine silica network spans the containing vessel. Of all the possible syntheses, the mixing of concentrated sulphuric acid and sodium silicate (i.e. water glass) to produce silica gel, through the formation of siloxane (–Si–O–Si–) bonds, has the largest industrial significance owing to the large-scale production of silica gel for every day applications such as an abrasive, filling and refining agent. Hence, although possessing an ill-defined starting point by virtue of having a range of initial species [1], it is perhaps somewhat surpris-

^{*} Corresponding author. Fax: +44-141-552-2891; e-mail: djs.birch@strath.ac.uk

ing that silica hydrogel dynamics have received such little attention in the research literature. Over the past two decades the picture has emerged of acidic silica hydrogels (i.e. at $\text{pH} < 2$) being formed by the coalescence of nanometer-scale polymer particles containing ~ 4 or 5 silica tetrahedra [2] to form secondary particles rather than through the extension and cross-linking of polymer chains as is the case for organic polymers [1]. Brinker and Scherer [1] have documented the effect of pH and surface charge on t_g and particle growth. At $\text{pH} \approx 2$ the surface charge is neutral, becoming slightly positive at $\text{pH} < 2$ (acidic gels), resulting in long gel times and little particle growth other than through aggregation. The surface charge is negative at $\text{pH} > 2$, facilitating more rapid gelation up to pH 6. At $\text{pH} > 7$ particles are highly anionic, mutually repulsive, form stable sols and grow mainly by the dissolution of smaller particles and deposition of silica on larger particles due to solubility differences (Ostwald ripening).

Considerable effort has been applied to solutions of Smoluchowski's equation and computer simulations in order to model cluster growth [1]. Reaction- or diffusion-limited cluster-cluster aggregation (RLCA or DLCA, respectively) models [3], modified to take account of deformation due to rearrangement about the point of initial contact between clusters [4], have proved successful at describing the kinetic and structural processes prior to gelation. At $\text{pH} < 2$, the slightly positive repulsion between particles which bind on collision according to the probability of an inter-particle condensation reaction is thought to lead to RLCA conditions which predicts growth [1] for non-gelling systems described by a mean diameter $d \approx \exp(ct)$. Conversely, DLCA predicts $d \approx t$. The lack of primary particle growth other than by aggregation at low pH makes acidic hydrogels ideal for studying cluster dynamics. However, the small size of primary particles makes the task difficult as sub-nm resolution is required to answer fundamental questions concerning silica hydrogelation and inter alia silica particle dimensions. For example, at what point are silica primary particles formed in the sol or are they already present in the silicate? What is the rate of change of particle size during polymerisation? Is there a relationship between particle size, gelation time and silicate concentration? We have sought to answer such questions by time-resolved fluorescence

measurements on silica particles labelled with a fluorescent dye.

Changes in the decay of fluorescence anisotropy as polymerisation proceeds are simply explained in terms of changes in the relative abundance of solvated dye and dye attached to silica particles. This dual behaviour of the probe means that a single anisotropy decay measurement leads to determination of both the fluid microviscosity and the particle hydrodynamic diameter. Although microviscosity in silicon alkoxide alcogels has recently been studied using fluorescence anisotropy [5,6], no evidence for particles was reported. Also, fluorescence studies of silica hydrogels at $\text{pH} < 2$ are more difficult than for alkoxide alcogels because of hydrogel intrinsic fluorescence and highly acidic nature which can lead to chemical degradation of aromatic probes. We have overcome these problems using the xanthene type probe JA120 [7,8], which has fluorescence characteristics unperturbed by this harsh environment. The near-infrared fluorescence of this dye (spectral peak at 690 nm) brings additional benefits. Specifically, reduced Rayleigh scattering of excitation and fluorescence (λ^{-4} dependence), negligible sol-gel intrinsic fluorescence and compatibility with diode laser excitation, such that fluorescence decays can be accurately measured in ~ 2 min time windows, during which time any change in the sol-gel is minimised.

Different weight for weight (w/w) concentrations of sulphuric acid and silicate (Crystal 79) were mixed together using stainless-steel blades rotating at 1200 rpm and delivered at controlled flow rates using peristaltic pumps to produce specific sol-gels of differing t_g . For the results presented here the particle surface charge was kept effectively constant by keeping the excess acid normality in the final sol in the range between 0.25 and 0.31 N (pH 0.9 to 0.81, respectively). The t_g for the sol compositions studied varied between ~ 60 and 3000 min. Orthogonal polarised fluorescence decay curves were each recorded in ~ 1 min, at different time delays following initial mixing of the sol using the time-correlated single-photon counting technique [9]. Excitation was provided by a Hamamatsu PLP-02 650 nm diode laser generating vertically polarised optical pulses of duration ~ 50 ps at 1 MHz repetition rate. The detector was an EG&G CD2027 avalanche photodiode. The overall instrumental response function was

~ 350 ps fwhm. Fluorescence was selected using IBH Model 5000 M f/3 monochromator, a Kodak 720 nm cut-off filter and a Halbro Optics dichroic polariser. Non-linear least-squares impulse resolution analysis of the anisotropy data [9] was performed using the IBH Fluorescence Lifetime Systems software library with a chi-squared, χ^2 , goodness of fit criterion. For all the measurements ~ 4 cm³ of sol remained optically transparent in $1 \times 1 \times 4$ cm unsealed cuvettes as gelation and drying occurred, such that depolarisation due to multiple scattering from particles and pores can be neglected.

Fluorescence depolarisation can be represented by the reorientational correlation function [10] $r(t) = 0.4\langle P_2[\mu_e(t)\mu_a(0)] \rangle$, where $\mu_e(t)$ and $\mu_a(0)$ are the emission and absorption dipoles at time t and time zero, respectively, and P_2 is the second-order Legendre polynomial. A dye bound to a silica particle can be described well by the Brownian isotropic rotation of a sphere, such that the usual three diffusion tensors are reduced to one, D , giving the Perrin equation for the decay of fluorescence anisotropy [11]

$$r(t) = r_0 \exp(-6Dt), \quad (1)$$

where r_0 is the initial anisotropy with a maximum value of 0.4 and, in the simplest case, the rotational correlation time τ_r is described by the Stokes–Einstein equation

$$\tau_r = (6D)^{-1} = \eta V/kT, \quad (2)$$

where η is the microviscosity, V the hydrodynamic volume, T temperature and k Boltzmann constant. By recording vertically and horizontally polarised fluorescence decay curves, $F_V(t)$ and $F_H(t)$, orthogonal to vertically polarised excitation, an anisotropy function $r(t) = [F_V(t) - F_H(t)]/[F_V(t) + 2F_H(t)]$ can be generated.

Our study of JA120 in a range of solvents showed it to be an isotropic rotor with a hydrodynamic radius of 3.5 Å [8]; a figure we have used in subsequent viscosity calculations. JA120 is cationic and at the pH used in our measurements (< 1) the silica particles are slightly positive. This slight repulsion of the dye by the silica leads to a fraction f of the total fluorescence being due to the probe molecules bound to silica particles and hence $1 - f$

due to probe molecules unbound in the sol. The anisotropy then takes the form

$$r(t) = (1 - f)r_0 \exp(-t/\tau_{r1}) + fr_0 \exp(-t/\tau_{r2}), \quad (3)$$

with τ_{r2} giving the particle diameter, which can be derived from Eq. (2) after using τ_{r1} to determine the microviscosity of the aqueous phase of the sol.

Fig. 1 shows typical anisotropy decay curves, illustrating the trends observed as polymerisation proceeds for a 15.3% by weight SiO₂ concentration. Distinguishing between alternative kinetic models of two rotational correlation times and zero residual anisotropy (Eq. (3)) and one rotational time and a non-zero residual anisotropy (Eq. (4)) can be difficult to establish in a single measurement [8].

$$r(t) = (r_0 - r_\infty)\exp(-t/\tau_r) + r_\infty. \quad (4)$$

Eqs. (3) and (4) are not necessarily mutually exclusive because, on longer time scales than we are able to observe the anisotropy with reasonable statistical precision (~ 20 ns), a long rotational time could be equally well described by a residual anisotropy. This is because anisotropy information is only available during the short fluorescence decay of JA120 (lifetime on silica particles typically increasing from ~ 2.5 to 2.8 ns during gelation [8]). However, for the four sols reported here, fitting to Eq. (3) consistently gave a better description (lower χ^2 value) than Eq. (4) (in total ~ 100 anisotropy decay measurements). Table 1 clearly supports this conclusion. Also,

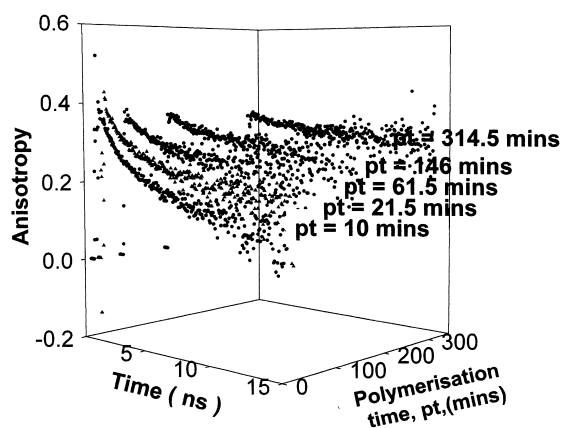


Fig. 1. Fluorescence anisotropy decay curves as function of polymerisation time, pt, for a 15.3% SiO₂ and 0.27 N sol–gel.

Table 1
Kinetic analysis of a 12.70% SiO₂, 0.25 N sol–gel

| Time | Fitting to Eq. (3) | | | | | Fitting to Eq. (4) | | | |
|--------|------------------------|-----------------------|-------|------|----------|-----------------------|-------|------------|----------|
| | τ_{r_1} (s) | τ_{r_2} (s) | r_0 | f | χ^2 | τ_r (s) | r_0 | r_∞ | χ^2 |
| 17.5 | 6.92×10^{-10} | 1.34×10^{-8} | 0.38 | 0.61 | 1.02 | 1.98×10^{-9} | 0.34 | 0.13 | 1.33 |
| 28 | 5.63×10^{-10} | 1.56×10^{-8} | 0.39 | 0.65 | 1.18 | 2.15×10^{-9} | 0.35 | 0.15 | 1.62 |
| 36 | 7.82×10^{-10} | 1.99×10^{-8} | 0.37 | 0.69 | 1.09 | 2.39×10^{-9} | 0.34 | 0.17 | 1.39 |
| 48 | 8.16×10^{-10} | 2.32×10^{-8} | 0.37 | 0.69 | 1.06 | 2.35×10^{-9} | 0.34 | 0.18 | 1.30 |
| 57.5 | 5.52×10^{-10} | 2.16×10^{-8} | 0.38 | 0.73 | 1.06 | 2.66×10^{-9} | 0.34 | 0.19 | 1.39 |
| 70 | 6.69×10^{-10} | 2.62×10^{-8} | 0.38 | 0.73 | 1.10 | 2.44×10^{-9} | 0.35 | 0.20 | 1.39 |
| 78 | 5.55×10^{-10} | 2.57×10^{-8} | 0.38 | 0.74 | 1.02 | 2.72×10^{-9} | 0.34 | 0.20 | 1.37 |
| 88.5 | 5.30×10^{-10} | 2.71×10^{-8} | 0.38 | 0.77 | 1.00 | 3.13×10^{-9} | 0.34 | 0.21 | 1.43 |
| 109 | 5.39×10^{-10} | 3.21×10^{-8} | 0.37 | 0.77 | 1.05 | 2.72×10^{-9} | 0.34 | 0.22 | 1.35 |
| 125 | 5.56×10^{-10} | 3.63×10^{-8} | 0.37 | 0.79 | 0.97 | 2.71×10^{-9} | 0.34 | 0.23 | 1.22 |
| 133.5 | 7.25×10^{-10} | 3.81×10^{-8} | 0.37 | 0.80 | 1.09 | 2.87×10^{-9} | 0.34 | 0.23 | 1.31 |
| 165 | 5.37×10^{-10} | 4.60×10^{-8} | 0.37 | 0.80 | 1.16 | 2.51×10^{-9} | 0.34 | 0.25 | 1.33 |
| 265 | 5.28×10^{-10} | 6.30×10^{-8} | 0.36 | 0.85 | 0.97 | 2.75×10^{-9} | 0.34 | 0.27 | 1.13 |
| 278 | 2.73×10^{-10} | 5.90×10^{-8} | 0.39 | 0.81 | 1.07 | 2.77×10^{-9} | 0.34 | 0.27 | 1.32 |
| 305.5 | 5.77×10^{-10} | 7.65×10^{-8} | 0.36 | 0.86 | 1.11 | 2.35×10^{-9} | 0.34 | 0.28 | 1.24 |
| 370.5 | 3.99×10^{-10} | 6.87×10^{-8} | 0.37 | 0.86 | 1.17 | 2.94×10^{-9} | 0.34 | 0.28 | 1.38 |
| 1709.5 | 1.52×10^{-10} | 1.19×10^{-7} | 0.41 | 0.87 | 0.93 | 1.07×10^{-8} | 0.36 | 0.30 | 1.00 |
| 4223 | 5.39×10^{-10} | 7.82×10^{-8} | 0.34 | 0.95 | 1.13 | 1.90×10^{-8} | 0.33 | 0.22 | 1.18 |
| 7250 | 5.36×10^{-10} | 8.31×10^{-8} | 0.39 | 0.96 | 1.09 | 3.02×10^{-8} | 0.38 | 0.20 | 1.10 |
| 8860 | 5.34×10^{-10} | 7.28×10^{-8} | 0.38 | 0.96 | 1.02 | 2.52×10^{-8} | 0.37 | 0.21 | 1.04 |
| 9975 | 1.02×10^{-10} | 7.21×10^{-8} | 0.39 | 0.95 | 1.04 | 2.07×10^{-6} | 0.34 | −9.50 | 1.14 |
| 13011 | 5.25×10^{-10} | 7.05×10^{-8} | 0.36 | 0.96 | 1.04 | 4.18×10^{-7} | 0.35 | −1.80 | 1.07 |

Eq. (3) was found to provide r_0 values closest to the theoretical maximum of 0.4 and which are reassuringly constant as f increases with time (cf. Table 1). Moreover, extension of Eq. (3) to include a fraction of fluorescence, due to dye bound to the macro-network in the gel was found to be inappropriate. Fortunately, the fluorescence lifetime of JA120 in the liquid phase (~ 1.8 ns) is sufficiently close to that in silica for the simplified anisotropy analysis we have used to be a reasonable approximation. Certainly none of the anisotropy decay curves we have measured pass through a minimum, which would be indicative of heterogeneous environments with a significant difference in fluorescence lifetime, i.e., we can neglect any time dependence of f during the fluorescence decay.

Precipitating silica at various times during the sol to gel transition, by the addition of excess methanol, confirmed the probe to be both free in solution and attached to silica with more dye recovered in the methanol filtrate at earlier times. Fig. 1 shows the

relative fluorescence intensity f due to the long rotational correlation time increases with polymerisation time. These facts confirm the fluorescence anisotropy reflects the joint contributions of unbound probe rotating in the fluid and probe bound to silica particles. At long times nearly all the emission originates from dye bound to silica particles and Eq. (1) then gives quite a good fit to the anisotropy decay. We observed the total fluorescence count rate to increase during polymerisation ($\sim 30\%$) and this probably reflects an increase in fluorescence quantum yield when the dye is bound to silica. For this reason the fraction f does not describe the fraction of the total number of probe molecules which are bound to silica.

Turning now to the rotational correlation times determined with Eq. (3). For a given sol, τ_{r_1} was fairly constant within the range ~ 0.5 to 1 ns and this constancy within the error is illustrated in Fig. 2 for the corresponding microviscosity; derived from Eq. (2) to be in the range ~ 1 to 2 cP. We associate

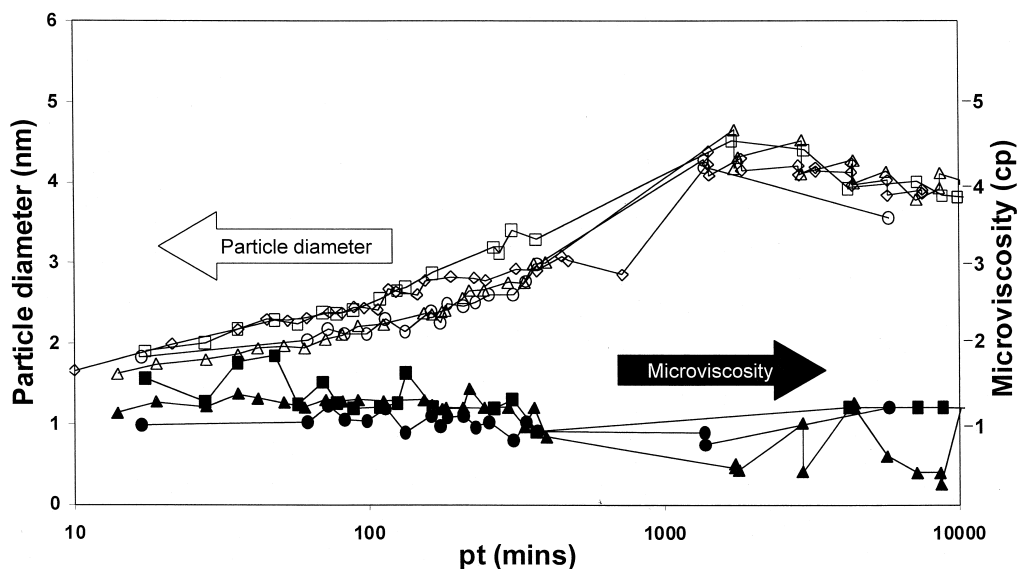


Fig. 2. Fluid microviscosity (solid symbols) and particle hydrodynamic mean diameter (open symbols) as a function of polymerisation time, pt , for 15.3% final SiO_2 concentration and 0.27 N excess acid normality (viscosity omitted for clarity, diameter \diamond), 12.7% SiO_2 and 0.25 N (\blacksquare , \square), 9.14% SiO_2 and 0.31 N (\blacktriangle , \triangle), and 6.02% SiO_2 and 0.30 N (\bullet , \circ) sol-gels. The corresponding t_g values are 60–74, 240–270, 990–1050, and 2760–3240 min, respectively.

τ_{r_1} with the rotation of the probe in the fluid part of the sol and indeed in residual fluid in the gel. Hence the microviscosity is significantly less than the bulk viscosity at all times and our interpretation finds no evidence for the coexistence of two viscosity domains as reported in alkoxide alcogels [6]. Because the fraction of fluorescence from free dye decreases with time the error in the microviscosity increases. Nevertheless there is some evidence in our data that the microviscosity is lowered during polymerisation, consistent with the take-up of silicate species from the fluid.

Fig. 2 also shows how the mean particle hydrodynamic diameter changes from the outset. From τ_{r_1} we have fitted to the microviscosity measurements in the temporal regions where they prevail for each sol and hence determined particle diameters from τ_{r_2} using Eq. (2). The maximum mean hydrodynamic diameter of particles existing initially or formed within 20 min of mixing is ~ 1.5 nm. We say maximum because we have made no allowance for the dimensions of the dye (~ 0.7 nm). However, the dye might be expected to intercalate within the open

form of such primary structures [1], thus adding little to the cluster diameter. Also, we have made no allowance for water molecules associated with the silica particles. The question then arises as to whether or not we can determine silica particle rotational times as long as 20–100 ns, shown in Table 1, with the short fluorescence lifetime of JA120 (~ 2.8 ns). Prior to this work our first reaction would have been to think not. However, the monotonic change in τ_{r_2} with time and better fit to Eq. (3) over all the compositions studied give us confidence in this interpretation. The increase in f with time helps us here. It is worth noting that we have reproduced the silica growth curves reported here using another xanthene type dye, JA53, with a hydrodynamic radius of 2.8 \AA [7]. Both JA120 and JA53 contain a carboxylic acid functional group which is likely to undergo a condensation reaction with silanol groups to produce the dye take-up by silica particles.

A striking feature of Fig. 2 is the near \AA resolution of the mean particle diameter, increasing from a minimum of ~ 1.5 nm to a peak of ~ 4.5 nm in ~ 2000 min and then decreasing to ~ 4 nm in

~ 6000 min for all the sols. This suggests the 4.5 nm clusters contain a maximum of ~ 13 primary particles [12].

Unsealed cuvettes containing silica hydrogels typically show a 40% loss in weight due to water evaporation after one week from preparation. Although the increasing depolarisation after 2000 min might be explained by an anomaly caused by depolarisation due to dye–dye Förster non-radiative resonance energy transfer [9] if the dye aggregates, throughout the polymerisation process we found no change in absorption spectrum of the dye as would be indicative of dye clustering. Also, the rate of decay of anisotropy is constant after ~ 6000 min despite the gel still drying and this is inconsistent with Förster energy transfer. In any case, the primary particle:dye number density was ~ 10⁵:1 for all the sols studied. Particle size reduction due to re-dissolution of silica seems unlikely (Ostwald ripening contributing little to the growth of primary particles at low pH [1]). Nor do we see why either sieve deposition of the larger particles in the gel or reduction in the hydration sphere would be significant. Because errors in individual microviscosity measurements are quite large at later times, due to f increasing, we studied the effect of a wide range of possible microviscosities on the calculated diameter. A decrease in silica particle diameter at later times was still observed in all cases. Hence we propose the size decrease we observe reflects the dominance of intra-particle syneresis over inter-particle aggregation. Syneresis is a term more usually applied to gels, but at the molecular level it involves, in the simplest form, shrinkage via conversion of monosilicic acid, Si(OH)₄, to siloxane, –Si–O–Si–, bridging bonds through polycondensation reactions [1], (i.e., ≡Si–OH + OH–Si≡ → ≡Si–O–Si≡ + H₂O). Particle syneresis probably occurs from the outset, but is hidden at earlier times by aggregation. This implies that aggregation numbers for silica primary particles treated as solid spheres [12] may be slight underestimates. The aggregation rate would be expected to slow down as the number of particles decreases and the rate of particle syneresis slows down as all but any isolated hydroxyl groups are used up. Although not obvious on the log t axis of Fig. 2, the increase in particle mean diameter is initially described to a first-order approximation by $d \approx d_0 + (d_{\max} - d_0)$

$[1 - \exp(-kt)]$, with d_0 values attributable to primary particles ranging from 1.4 to 1.7 nm (uncorrelated with [SiO₂]). The rate parameter k is ~ 3.3 × 10⁻⁵, 6.0 × 10⁻⁵, 8.7 × 10⁻⁵ and 1.7 × 10⁻⁴ s⁻¹ for 6.02%, 9.14%, 12.7% and 15.3% SiO₂ (w/w), respectively. Just before d_{\max} the net k value is reduced by syneresis. The particle syneresis rate constant, assuming an exponential reduction in particle diameter and that growth is absent after 30 h, is ~ 6.0 × 10⁻⁶ s⁻¹. Particle syneresis is seen to be effectively over after ~ 100 h. The ‘life history’ of silica particles during hydrogel polymerisation is summarised according to our results in Fig. 3.

Only the growth rate k , but not d_0 or d_{\max} has any measurable dependence on [SiO₂] or t_g ; at t_g the sol still being much more abundant than the gel. The d_0 value of ~ 1.5 nm which we detect is in close agreement with values reported from small angle scattering measurements made in many different laboratories over a range of sol–gel samples. For example, light scattering measurements on a silicon alkoxide sol found a primary particle hydrodynamic diameter of 1.0 nm, increasing to 2.4 nm prior to gelation [13]. Small-angle X-ray scattering studies of silica gel have revealed evidence for 1 nm particles [14] and similar studies on another alkoxide sol indicate that 2 nm diameter primary particles aggregate to form secondary particles of 6 nm diameter prior to gelation [15]. Small-angle neutron scattering has produced comparable primary particle dimensions [16]. In one of the few studies on silica hydrogel formation, primary particles of ~ 1 nm have been detected using X-ray scattering [17].

Similar particle growth curves to what we observe have been reported using electron microscopy on base catalysed silicon alkoxide sols, but from an initial measurement of ~ 100 nm [18], which means the growth function of the ~ 1 nm primary particles was still not resolved. By choosing polymerisation conditions which have a slow aggregation rate we have been able to observe primary particle growth from the outset and secondary particle syneresis against a background gel network. The condensation mechanism of growth and syneresis suggest these new observations are fundamental to sol–gel kinetics in general. Moreover, growth curves such as Fig. 2 should be useful in controlling the surface area of silica gel by stopping the polymerisation at a given

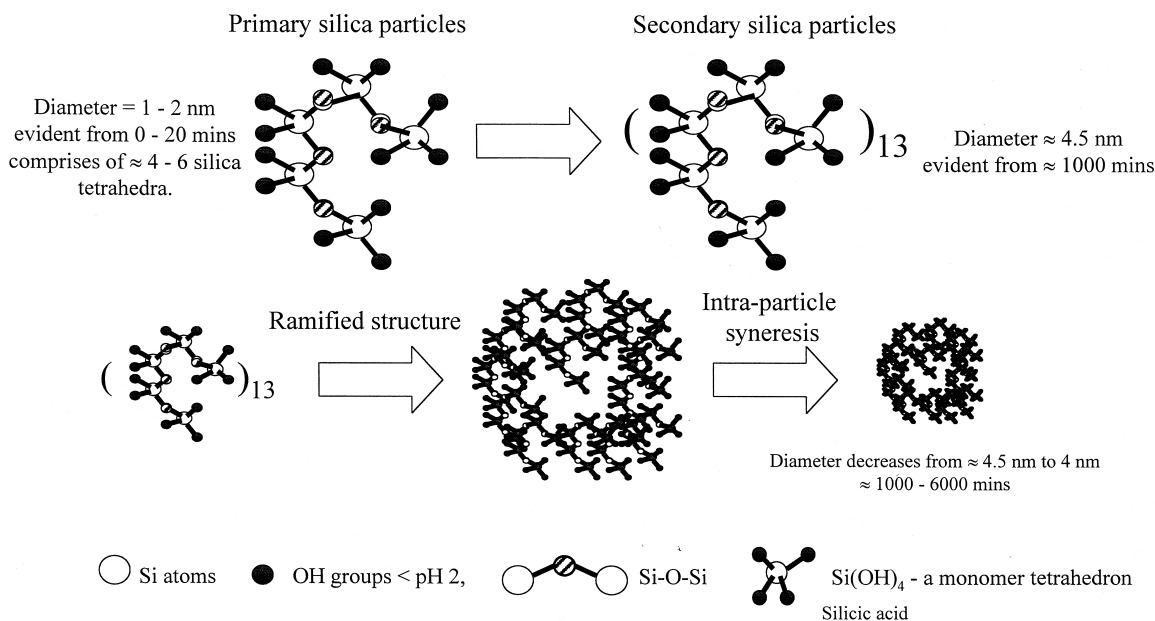
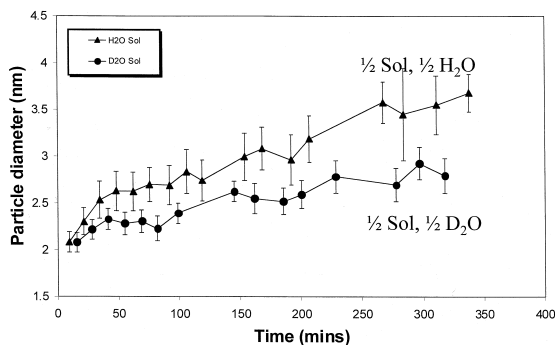


Fig. 3. Changes in silica particle size during hydrogel polymerisation.

time and hence halting further particle growth (e.g., by adding an organic solvent). As a further demonstration of the resolution and application of the method we have described, we investigated the effect of adding D_2O and inorganic salts. For a 15.1% (w/w) final SiO_2 concentration at pH 0.76, 1.5 ml of the sol was diluted with an equal volume of doubly distilled demineralised water and another 1.5 ml of sol diluted with an equal volume of D_2O . The corresponding t_g values were 21 ± 1 and 26 ± 1.5 h, respectively. Fig. 4 shows that the hydrodynamic diameter and growth rate k is reduced on addition of

Fig. 4. The effect of D_2O on silica particle growth.

D_2O . The difference in particle diameter at ~ 200 min, could be caused by a reduction in hydrogen bonding on adding D_2O , corresponding to ~ 2 water molecules, solubility differences during early ripen-

Table 2

Effect of inorganic salt addition on the initial primary particle diameter, d_0 , and the rate of silica particle aggregate growth, k t_g -macrogelation time (the time for the liquid, the 'sol', to set firm)

| Sol-gel/added salts | d_0 (nm) | k (s^{-1}) | t_g (min) |
|---|---------------|----------------------------|----------------|
| 5.94% SiO_2 , 0.29 N (pure sol) ^a | 1.8 | 2.4×10^{-5} | 2803–3013 |
| 5.94% SiO_2 , 0.29 N (0.1 M NaCl) | 1.8 | 3.4×10^{-5} | 2743–2833 |
| 5.94% SiO_2 , 0.29 N (1 M NaCl) | 1.7 | 3.9×10^{-5} | 1823–1883 |
| 5.92% SiO_2 , 0.26 N (pure sol) ^a | 1.7 | 2.3×10^{-5} | 2895–3045 |
| 5.92% SiO_2 , 0.26 N (0.1 M NaNO_3) | 1.7 | 2.3×10^{-5} | 2820–2910 |
| 5.92% SiO_2 , 0.26 N (1 M NaNO_3) | 1.7 | 2.5×10^{-5} | 2580–2640 |

^a Both the 5.94% SiO_2 , 0.29 N and the 5.92% SiO_2 , 0.26 N sol-gels can be considered equivalent for comparison purposes.

ing, or the viscosity differences of the sol (1.26 cP for H₂O addition as compared to 1.59 cP for D₂O addition) influencing the relative diffusion rates of silica particles. Salts are well known to reduce t_g in sol–gel systems [1]. Table 2 shows that for acidic silica hydrogels the addition of salt has little effect on d_0 , but a measurable effect on k in the case of NaCl-doped sol–gels.

The method we have described is in some ways much better placed than conventional techniques to record particle size in situ at high silicate concentrations and after gelation. Fluorescence depolarisation is only caused by rotating particles. Conversely, to avoid multiple scattering, light scattering requires dilute silicates (dilution can cause depolymerisation) and X-ray, neutron and light scattering also occur from the gel network as well as particles. The technique we have described can be used for particle size measurement in any type of sol provided a suitable bound dye can be found, the maximum size of particle which can be resolved being determined only by the fluorescence lifetime of the dye. Of course we are only measuring the mean of what is undoubtedly a distribution of diameters, but distribution analysis may even be possible. Full details of our findings, including pH studies, will be reported shortly.

Acknowledgements

We wish to acknowledge the EPSRC for research grants including a Post Doctoral Research Fellowship held by C.D.G., the gift of JA120 kindly made available to us by Dr. Jutta Arden-Jacob, University of Seigen, Germany, and technical support by J.

Revie in helping to construct the sol–gel preparation rig. The comments and support of D. Ward of Unilever plc and D. Aldcroft, I. McKeown, N. Rhodes and A. Minihan of Crosfield are gratefully acknowledged.

References

- [1] C.J. Brinker, G. Scherer, *Sol–Gel Science, The Physics and Chemistry of Sol–Gel Processing*, Academic Press, San Diego, CA, 1989.
- [2] J.K. West, B.F. Zhu, Y.C. Cheng, L. Hench, *J. Non-Cryst. Solids* 121 (1990) 51.
- [3] P. Meakin, *Phys. Rev. Lett.* 51 (1983) 1119.
- [4] R. Jullien, A. Hasmy, *Phys. Rev. Lett.* 74 (1995) 4003.
- [5] B. Dunn, J.I. Zink, *J. Mater. Chem.* 1 (1991) 903.
- [6] F.V. Bright, U. Narang, R. Wang, P.N. Prasad, *J. Phys. Chem.* 98 (1994) 17.
- [7] K.H. Drexhage, N.J. Marx, J. Arden-Jacob, *J. Fluoresc.* 7 (1997) 91s.
- [8] C.D. Geddes, J.M. Chevers, D.J.S. Birch, *J. Fluoresc.* 9 (1999) 73.
- [9] D.J.S. Birch, R.E. Imhof, in: J.R. Lakowicz (Ed.), *Topics in Fluorescence Spectroscopy*, Vol. 1, Plenum, New York, 1991, p. 1.
- [10] A. Szabo, *J. Chem. Phys.* 81 (1984) 150.
- [11] A. Kawski, *Crit. Rev. Anal. Chem.* 23 (1993) 459.
- [12] D.E.G. Williams, *J. Non-Cryst. Solids* 86 (1986) 1.
- [13] A.H. Boonstra, T.P.M. Meeuwssen, J.M.E. Baken, G.V.A. Aben, *J. Non-Cryst. Solids* 109 (1989) 153.
- [14] B. Himmel, Th. Gerber, H. Bürger, *J. Non-Cryst. Solids* 91 (1987) 122.
- [15] G. OrceI, L.L. Hench, I. Artaki, J. Jonas, T.W. Zerda, *J. Non-Cryst. Solids* 105 (1988) 223.
- [16] R. Winter, D.-W. Hua, P. Thiyagarajan, J. Jonas, *J. Non-Cryst. Solids* 108 (1989) 137.
- [17] Th. Gerber, B. Himmel, C. Hübert, *J. Non-Cryst. Solids* 175 (1994) 160.
- [18] G.H. Bogush, C.F. Zukoski, *J. Colloid Interface Sci.* 142 (1991) 1.